

Effects of bedding on hydraulic fracturing in coalbed methane reservoirs

Tingting Jiang, Jianhua Zhang*, Gang Huang, Shaoxian Song and Hao Wu*

Hubei Province Key Laboratory of Processing of Mineral Resources and Environment, School of Resource and Environmental Engineering, Wuhan University of Technology, Wuhan 430070, Hubei, China

Bedding is a special structure of coal, which has notable effects on the mechanical parameters of coal and on the hydraulic fracture propagating in coalbed methane reservoirs. To study the effects of bedding on anisotropic characteristics of coal fracture toughness, three-point bending tests have been carried out on raw coal specimens. The results indicate that fracture toughness and failure modes of the specimens both have strong anisotropy due to bedding. A geological geomechanical model of a coalbed methane (CBM) reservoir is built taking into account the effect of bedding to study the hydraulic fracture propagation and the influence of bedding on the fracture network. The hydraulic fracture initiates at the end of the perforation and tends to bifurcate and swerve at the bedding to produce induced fractures. Ultimately, these fractures form a complicated fracture network. The fracture toughness of bedding has great influence on hydraulic fracture geometry. The fracture is likely to bifurcate and swerve at the bedding to form multiple secondary fractures with larger bedding fracture toughness.

Keywords: Coalbed methane, coal seam, fracture toughness, hydraulic fracturing, numerical simulation, three point bending test.

In coalbed methane (CBM) reservoirs the bedding always fractures before the matrix for its weak cementation^{1,2}. This has a significant impact on the reservoir exploitation, mechanical properties, stress distribution of borehole surrounding rock and crack initiation^{3,4}. Complex fracture geometry can be formed at bedding during hydraulic fracture propagation^{5,6}. Therefore, it is of great significance to study the effects of bedding on hydraulic fracture propagation in CBM reservoirs. Several studies have been carried out in related fields.

Jeffrey *et al.*⁷ studied the influence of bedding, face cleats and joints on the fracture geometry. Gu *et al.*⁸ proposed an interfacial slip model based on the displacement discontinuity method. Cho *et al.*⁹ studied the influence of transverse isotropic plane on deformation and strength anisotropy of Boryeong shale. Liu *et al.*¹⁰ comprehensively studied the influence of horizontal bedding on ten-

sile and compressive mechanical properties in a coal seam. Guo *et al.*¹¹ confirmed that a fracture network can be easily formed in shale when hydraulic fracture does not extend along the natural bedding plane. Heng *et al.*¹² studied the effect of bedding plane orientations on shear strength of shale. Jiang *et al.*¹³ simulated hydraulic fracturing by carrying out true triaxial tests on cubic raw coal specimens. Ma *et al.*¹⁴ studied the effect of bedding on the anisotropic permeability of shale. Zou *et al.*¹⁵ concluded the bedding had notable effects on injection pressure and hydraulic fracture height during hydraulic fracturing in shale formation. However, the effects of bedding on hydraulic fracturing in CBM reservoirs are relatively rare. This leads to the effects of bedding on the fracturing in CBM reservoirs not being well understood.

On account of the complex structural characteristics of bedding in CBM reservoirs, the anisotropy of mode I fracture toughness is analysed based on stress field distribution characteristics of a crack tip in an anisotropic material. Three-point bending tests have been carried out on samples cored from Jiaozuo coal mine. The mechanical properties are obtained and the effects of bedding on the anisotropic characteristics of the coal seam are investigated. To study the effects of bedding on the hydraulic fracturing, a geological geo-mechanical model based on the target reservoir geological characteristic is developed using RFPA (realistic failure process analysis) software¹⁶. The propagation rules of cracks and the influence of bedding on the fracture network in a CBM reservoir are analysed. Research results can provide a reference to understand the important role of bedding in forming the network cracks in CBM reservoirs during hydraulic fracturing.

A CBM reservoir has the characteristic of strong brittleness and very poor plasticity. Hence the instability extension of a hydraulic fracture can be analysed based on linear elastic fracture mechanics (LEFM)¹⁷. Stress intensity factor is not only an important parameter to express the crack-tip stress, but an important index to judge the crack instability state in LEFM¹⁸. Therefore, it is of great significance to analyse the distribution characteristics of the crack-tip stress field in an anisotropic material, understand the anisotropy of coal rock fracture toughness, and further study the complex extension rule of a hydraulic fracture. Figure 1 shows the local coordinate

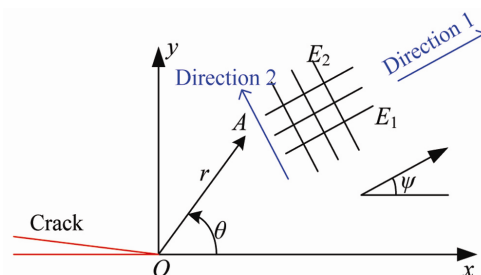


Figure 1. Crack tip diagram in an anisotropic material (the coordinates of point A are (r, θ)).

*For correspondence. (e-mail: zjhwt@sina.com; haowu1977@163.com)

diagram of the crack tip in an anisotropic material. The length of the fracture is $2a$.

The basic differential equation of the generalized plane stress problem is¹⁹

$$a_{11} \frac{\partial^4 F}{\partial y^4} + a_{22} \frac{\partial^4 F}{\partial x^4} - 2a_{26} \frac{\partial^4 F}{\partial x^3 \partial y} - 2a_{16} \frac{\partial^4 F}{\partial x \partial y^3} + (2a_{12} + a_{66}) \frac{\partial^4 F}{\partial x^2 \partial y^2} = 0, \quad (1)$$

where a_{ij} is flexibility coefficient and F is stress function of anisotropic material plane problems.

The basic differential equation of the generalized plane strain problem is obtained by replacing a_{ij} with β_{ij} . The relationship between β_{ij} and a_{ij} is

$$\beta_{ij} = a_{ij} - \frac{a_{i3}a_{j3}}{a_{33}}, \quad (2)$$

where β_{ij} is the reduction flexibility coefficient.

For orthotropic material, eq. (1) can be simplified as

$$\frac{1}{E_1} \frac{\partial^4 F}{\partial y^4} + \frac{1}{E_2} \frac{\partial^4 F}{\partial x^4} + \left(\frac{1}{G_{12}} - \frac{2\nu_2}{E_2} \right) \frac{\partial^4 F}{\partial x^2 \partial y^2} = 0, \quad (3)$$

where E_1 is the elasticity modulus in transverse isotropic plane, Pa; E_2 stands for the elasticity modulus perpendicular to E_1 , Pa; G_{12} is the shear modulus perpendicular to E_1 , Pa; ν_2 is the Poisson's ratio perpendicular to E_1 , Pa.

The asymptotic solutions of the crack tip stress field are²⁰

$$\left\{ \begin{aligned} \sigma_x &= \frac{K_I}{\sqrt{2\pi r}} \operatorname{Re} \left[\frac{\Sigma_1 \Sigma_2}{\Sigma_1 - \Sigma_2} \left(\frac{\Sigma_2}{\eta_2} - \frac{\Sigma_1}{\eta_1} \right) \right] \\ &+ \frac{K_{II}}{\sqrt{2\pi r}} \operatorname{Re} \left[\frac{1}{\Sigma_1 - \Sigma_2} \left(\frac{\Sigma_2^2}{\eta_2} - \frac{\Sigma_1^2}{\eta_1} \right) \right] \\ \sigma_y &= \frac{K_I}{\sqrt{2\pi r}} \operatorname{Re} \left[\frac{1}{\Sigma_1 - \Sigma_2} \left(\frac{\Sigma_2}{\eta_2} - \frac{\Sigma_1}{\eta_1} \right) \right] \\ &+ \frac{K_{II}}{\sqrt{2\pi r}} \operatorname{Re} \left[\frac{1}{\Sigma_1 - \Sigma_2} \left(\frac{1}{\eta_2} - \frac{1}{\eta_1} \right) \right] \\ \tau_{xy} &= \frac{K_I}{\sqrt{2\pi r}} \operatorname{Re} \left[\frac{\Sigma_1 \Sigma_2}{\Sigma_1 - \Sigma_2} \left(\frac{1}{\eta_1} - \frac{1}{\eta_2} \right) \right] \\ &+ \frac{K_{II}}{\sqrt{2\pi r}} \operatorname{Re} \left[\frac{1}{\Sigma_1 - \Sigma_2} \left(\frac{\Sigma_1}{\eta_1} - \frac{\Sigma_2}{\eta_2} \right) \right] \end{aligned} \right. \quad (4)$$

The asymptotic solutions of the crack tip displacement field are

$$\left\{ \begin{aligned} u &= K_I \sqrt{\frac{2r}{\pi}} \operatorname{Re} \left[\frac{1}{\Sigma_1 - \Sigma_2} (\Sigma_1 p_2 \eta_2 - \Sigma_2 p_1 \eta_1) \right] \\ &+ K_{II} \sqrt{\frac{2r}{\pi}} \operatorname{Re} \left[\frac{1}{\Sigma_1 - \Sigma_2} (p_2 \eta_2 - p_1 \eta_1) \right] \\ v &= K_I \sqrt{\frac{2r}{\pi}} \operatorname{Re} \left[\frac{1}{\Sigma_1 - \Sigma_2} (\Sigma_1 q_2 \eta_2 - \Sigma_2 q_1 \eta_1) \right] \\ &+ K_{II} \sqrt{\frac{2r}{\pi}} \operatorname{Re} \left[\frac{1}{\Sigma_1 - \Sigma_2} (q_2 \eta_2 - q_1 \eta_1) \right] \end{aligned} \right. \quad (5)$$

where

$$\left\{ \begin{aligned} p_i &= a'_{11} \Sigma_i^2 + a'_{12} - a'_{16} \Sigma_i \\ q_i &= a'_{12} \Sigma_i + \frac{a'_{22}}{\Sigma_i} - a'_{26} \end{aligned} \right., \quad i=1, 2. \quad (6)$$

$$\eta_i = \sqrt{\cos \theta + \Sigma_i \sin \theta}. \quad (7)$$

The relationships between a_{ij} and a'_{ij} are

$$a'_{11} = a_{11} \cos^4 \psi + (2a_{12} + a_{66}) \sin^2 \psi \cos^2 \psi + a_{22} \sin^4 \psi, \quad (8)$$

$$a'_{22} = a_{11} \sin^4 \psi + (2a_{12} + a_{66}) \sin^2 \psi \cos^2 \psi + a_{22} \cos^4 \psi, \quad (9)$$

$$a'_{12} = a_{12} + (a_{11} + a_{22} - 2a_{12} - a_{66}) \times \sin^2 \psi \cos^2 \psi, \quad (10)$$

$$a'_{66} = a_{66} + 4(a_{11} + a_{22} - 2a_{12} - a_{66}) \times \sin^2 \psi \cos^2 \psi, \quad (11)$$

$$a'_{16} = [a_{11} \cos^2 \psi - a_{22} \sin^2 \psi - (2a_{12} + a_{66}) \cos 2\psi / 2] \sin 2\psi, \quad (12)$$

$$a'_{26} = [a_{11} \sin^2 \psi - a_{22} \cos^2 \psi + (2a_{12} + a_{66}) \cos 2\psi / 2] \sin 2\psi, \quad (13)$$

where a'_{ij} is the flexibility coefficient under the local coordinate system $x-O-y$; K_I is mode I stress intensity factor, $\text{MPa m}^{0.5}$; K_{II} is mode II stress intensity factor, $\text{MPa m}^{0.5}$; ψ is the included angle of material main direction 1 and x axis, degree; Σ_i is the material characteristic parameter related to coordinate system, $i=1, 2$.

Equation (1) shows that: (1) The same as for an isotropic material, the crack tip stress in the anisotropic

material has the singularity of $r^{-1/2}$ on the condition of $r \rightarrow 0$, and stress field strength is also determined by the stress intensity factor. (2) The distribution of stress and the displacement field depend not only on θ , but also relate to the elastic coefficient of the anisotropic material. For the anisotropic material, anisotropy not only influences the distribution of stress and displacement, but also the intensity of stress field and displacement field, which means they affect the value of the stress intensity factor. The stress intensity factor can be expressed by fracture toughness which reflects crack instability and propagation ability²¹.

The stratum tends to develop shear fracture along initial fissure under the condition of certain formation characteristics (initial fissure, distribution characteristic and stress state), especially when the difference between maximum and minimum *in situ* stress is large, the angle between initial fissure and principal stress is about 30–60° and low viscosity fluid is injected. Even if a shear fracture appears first, the tension fractures along the fracture plane are still mainly formed during the fracture propagation. The unstable propagation of tensile cracks mainly occurs in the matrix. Therefore, we assume the hydraulic fracture extension is mainly the unstable propagation of a type I crack to discuss the hydraulic fracture propagation rules in CBM reservoirs. The fracture toughness of type I cracks only is considered to study its anisotropy in a coal seam.

From the previous analysis, the critical values of mode I stress intensity factor are the fracture toughness of principal directions 1 and 2 when ψ is 0° and 90° respectively. In direction 1 along and direction 2 perpendicular to bedding respectively, the corresponding fracture toughness values can be obtained by three-point bending tests.

All the coal samples are taken from the Shanxi group II coal seam in Jiaozuo coal mine of Henan province, China. The coal seam is very thick (the average thickness is about 9 m), and has simple structure and distributional stability. Its depth is about –1070 m to –1080 m.

To study the influence of bedding on coal fracture toughness and predict the micro fractures propagation process, we carried out three-point bending tests. Because of the anisotropy of the coal, the angles between drilling direction and bedding plane have been selected as 0° and 90°. Figure 2 is a schematic diagram of the directional coring. The dashed line indicates bedding.

The cylindrical specimens used in the tests have the diameter and height of 50 and 200 mm respectively. For the specimen notch we adopt a longitudinal notch form. Its depth and width are 20 and 1.5 mm respectively²².

A multi-functional rock testing system (RMT) is used to carry out three-point bending tests on raw coal specimens with different bedding angles. The samples are divided into two groups based on the relative location of bedding and notch plane. In one group the notch plane is perpendicular to the bedding, and in the other group the

notch plane is parallel to the bedding. Each condition of test is performed on at least three samples, and the average of the test result is taken.

The fracture toughness is given by²³

$$K_{IC} = 0.25 \left(\frac{S_d}{D} \right) \frac{P_{\max}}{D^{1.5}} y \left(\frac{a}{D} \right), \quad (14)$$

$$y \left(\frac{a}{D} \right) = \frac{12.75 \left(\frac{a}{D} \right)^{0.5} \left[1 + 19.65 \left(\frac{a}{D} \right)^{4.5} \right]^{0.5}}{\left(1 - \frac{a}{D} \right)^{0.25}}, \quad (15)$$

where K_{IC} is the fracture toughness, $\text{MPa m}^{0.5}$; S_d is the distance between two supporting points, which is 160 mm during tests; D stands for specimen diameter, mm; P_{\max} is the peak load, N; a is the notch depth, mm.

From eqs (14) and (15), fracture toughness depends only on sample dimensions, notch geometry and failure load. Based on calculation formulas, three-point bending test results are listed in Table 1.

Table 1 shows that fracture toughness is the largest ($0.364 \text{ MPa m}^{0.5}$) when the notch plane is perpendicular to bedding, which means that the matrix has maximum fracture toughness. The minimum fracture toughness is $0.120 \text{ MPa m}^{0.5}$, when the notch plane is parallel to bedding, which reveals that bedding is a weak interface. The former is about three times of latter, which fully reflects the anisotropy of coal fracture toughness. Based on the above test results, bedding has a weak ability to prevent fracture initiation and propagation. If a hydraulic fracture extends perpendicular to bedding, it is extremely likely to have bifurcation and diversion at the bedding.

Figure 3 shows three-point bending typical fracture styles for different orientations of notch plane and bedding. Coal specimens rupture mode basically shows two types of failure: (1) notch plane perpendicular to bedding. The fracture does not initiate at the tip of the notch.

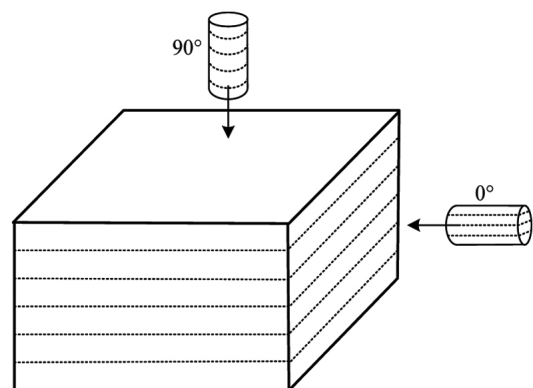


Figure 2. Directional coring schematic diagram.

Table 1. Three point bending test results

The relative position of notch plane and bedding	Notch depth/mm	Notch width/mm	Diameter/mm	Peak load/N	Fracture toughness/ MPa m ^{0.5}	Average value/ MPa m ^{0.5}
Perpendicular	18.92	1.58	49.61	562.72	0.409	0.364
	20.73	1.63	49.74	479.43	0.385	
	19.44	1.46	50.38	421.07	0.298	
Parallel	20.38	1.55	50.21	145.90	0.111	0.120
	20.15	1.57	49.82	177.04	0.136	
	19.27	1.66	49.65	151.27	0.112	

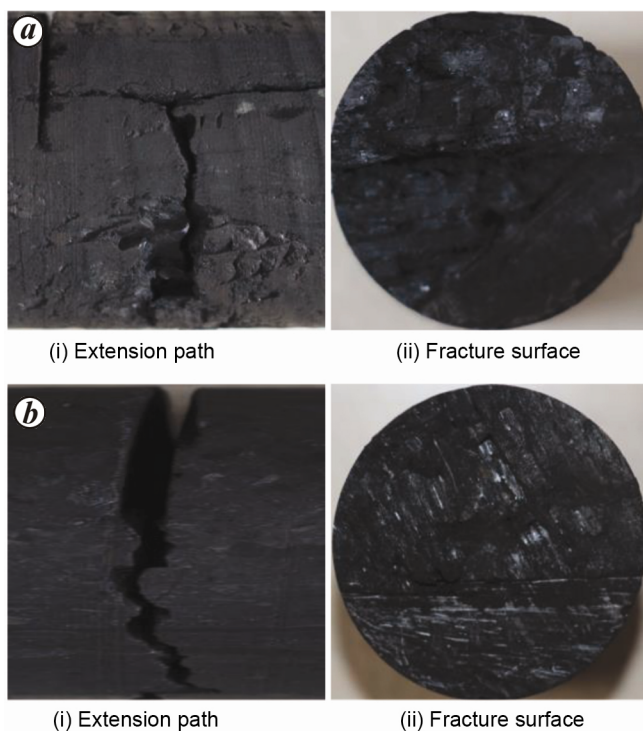


Figure 3. Fracture patterns of three point bending tests. *a*, Notch perpendicular to bedding. *b*, Notch parallel to bedding.

Instead it initiates along the bedding, near the notch tip. The fracture propagates along the bedding under the action of the applied load. A vertical diversion produces the secondary fracture, which propagates approximately parallel to the direction of notch depth. Ultimately, the broken sample contains two approximately vertical fractures. (2) Notch plane parallel to bedding. The fracture initiates at the tip of the notch and propagates along the prefabricated crack until complete break. It shows no deviation of fracture path. The failure sample forms a straight extension path, and the specimen breaks into two approximately equal parts. The fracture surface is the coal bedding, which is flat and smooth.

The main reason that causes the anisotropy of coal rock fracture toughness is the anisotropy of the toughening effect. For layered sedimentary rock, the main toughening mechanisms throughout the fracturing process are bed-

ding cracking, fracture path deviation and delamination peeling. When the notch is perpendicular to the bedding, bedding cracking and fracture path deviation are the reasons why fracture toughness has the maximum value during fracture propagation. When the notch is parallel to the bedding, the fracture propagates along bedding, which has no toughening mechanism. The bonding strength of bedding is low. Bedding has weak ability to prevent fracture extension, so fracture toughness has the minimum value.

A geological geomechanical model used to predict the propagation of fractures during hydraulic fracturing is built by finite element software RFPA¹⁶. The model is used to study the propagation rules of cracks and the influence of bedding on fracture network. Parameters used in numerical simulation are based on test results. The results can provide a reference basis for the fracture propagation rule and the geometry of fracture networks of CBM reservoirs during hydraulic fracturing.

To ensure that input parameters of the numerical model truly represent actual formation, the average values of coal rock matrix and bedding determined in laboratory tests are used. Table 2 lists the mechanical parameters of matrix and bedding.

According to geological data, the angle between bedding and horizontal plane is 18°–35°. To simplify the calculation, the angle is valued as 30° in numerical simulations. The hydraulic pressure is increased at a rate of 0.1 MPa by single steps until the stratum ruptures completely to form a number of hydraulic fracture channels. The fracturing fluid is water with the density and the injection rate of 1000 kg/m³ and 0.5 ml/s respectively.

Taking the cross-section perpendicular to wellbore as the research object, the calculation model of a well with perforation completion is established. The numerical model and its boundaries are shown in Figure 4. The model is a square with a side length of 10 m, and the wellbore diameter is about 0.2 m. The distance between the wellbore and the boundary is more than 10 times larger than the wellbore diameter, which could effectively reduce the boundary effect on the calculation results. There are 300 × 300 elements in the model, and the perforation depth is 150 mm, perpendicular to bedding. The horizontal *in situ* stresses are applied on two sides of the

model, and the displacement boundary is applied on the other two sides. The matrix and bedding are parallel and they alternate. The matrix is with a lighter colour and wider range, while the bedding has darker colour and narrower scope, as also marked in Figure 4. To reflect the actual characteristics of coal rock, the elasticity modulus of the model is not a fixed value to consider the influence of randomness.

The crack propagation in CBM reservoir during hydraulic fracturing is shown in Figure 5. With the fracturing fluid being injected into the formation continuously, the hydraulic fracturing cracks at both ends of the perforated interval and the fracture extends along the perforation direction (Figure 5 a). When the fracture extends to the bedding, bifurcation and diversion of the hydraulic fracture take place because of the low strength and high permeability of bedding. The induced fractures are produced along the bedding, while the major fracture still extends perpendicularly to the bedding, but with much lower fracture propagation speed (Figure 5 b).

Table 2. Parameters used in the simulation model

Items	Unit	Matrix	Bedding
Poisson's ratio		0.31	0.34
Internal friction angle	Degree	18.8	16.3
Elasticity modulus	GPa	1.93	0.65
Tensile strength	MPa	1.17	0.27
Cohesive strength	MPa	0.82	0.19
Permeability	mD	0.154	1.644
Porosity	%	4.8	3.8
Compressive strength	MPa	11.88	3.06
Fracture toughness	MPa m ^{0.5}	0.364	0.12
Vertical stress	MPa	23.4	
Maximum horizontal stress	MPa	25.7	
Minimum horizontal stress	MPa	16.7	

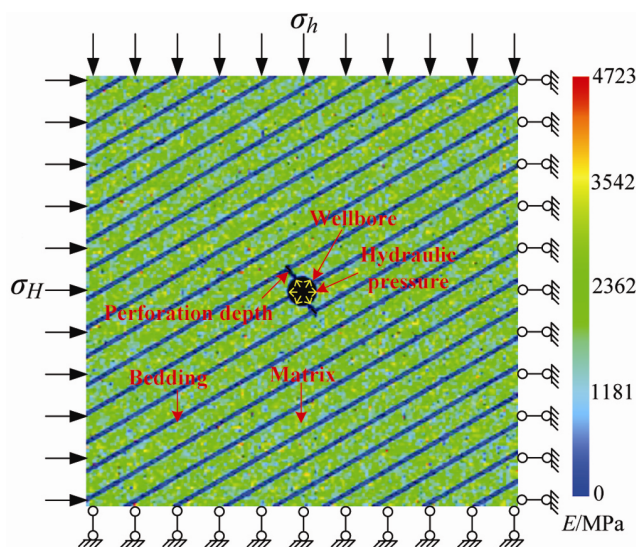


Figure 4. Two-dimensional plane strain model (E is elasticity modulus).

After the induced fracture propagates for a certain distance along the bedding, the fracturing fluid cannot maintain the rapid extension of the cracks because of high leak-off and energy consumed by the friction between the induced crack surfaces. So a new secondary fracturing crack forms along another bedding. The newly formed crack cannot stop the continuous extension of the major

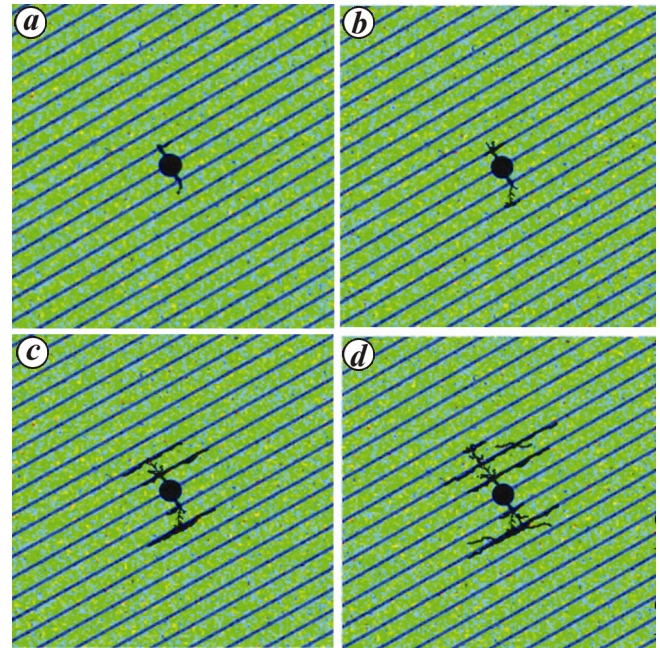


Figure 5. Hydraulic fractures evolution diagram at different injection pressures. *a*, 2.6 MPa; *b*, 2.8 MPa; *c*, 3.0 MPa; *d*, 3.2 MPa.

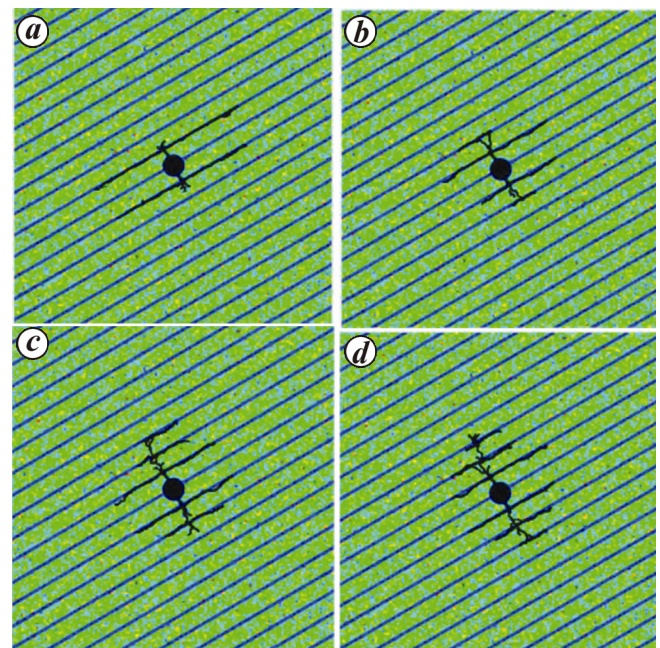


Figure 6. Hydraulic fracture morphology for different bedding fracture toughnesses. *a*, 0.05 MPa m^{0.5}; *b*, 0.1 MPa m^{0.5}; *c*, 0.15 MPa m^{0.5}; *d*, 0.2 MPa m^{0.5}.

fracture and the original secondary fractures completely but reduces their extension speed (Figure 5 c). Ultimately, the complex hydraulic crack network is formed which prevents the fast propagation of hydraulic fractures. Increasing the injection rate is the only way to ensure continuous and rapid extension of major and secondary fractures to form a more complicated fracture network (Figure 5 d).

To study the effects of fracture toughness of bedding on hydraulic fracture, the fracture toughness of bedding is taken as 0.05, 0.10, 0.15 and 0.20 MPa m^{0.5} respectively, while that of the matrix is set as 0.364 MPa m^{0.5}. The other parameters used in the simulations are listed in Table 2. The hydraulic fracture propagation geometry is shown in Figure 6.

As shown in Figure 6, the fracture toughness of bedding has great influence on hydraulic fracture geometry. When fracture toughness of bedding is larger, the hydraulic fracture is more likely to propagate perpendicular to the bedding, and the major fracture has bifurcation and diversion many times at the bedding to form multiple secondary fractures extending along bedding. With a decrease of bedding fracture toughness, the number of times of bifurcation and diversion at the bedding decreases, while the number of secondary fractures also gradually reduces. However, the propagation distance of secondary fractures along bedding increases gradually. This suggests that hydraulic fracture tends to propagate perpendicularly to the bedding, and has bifurcation and diversion to form complex fracture geometries on the condition of large fracture toughness of bedding. The secondary fracture tends to propagate along the bedding with simple fracture geometry on the condition of small fracture toughness of bedding. Therefore, hydraulic fracturing crack is likely to bifurcate and swerve at the bedding to form multiple secondary fractures in coal seam with larger bedding fracture toughness, which is beneficial to form a fracture network.

To summarize the results:

(1) The material anisotropy not only influences the distribution of stress and displacement at a crack tip, but also affects the intensities of stress field and displacement field, which are both determined by stress intensity factor and elastic constants.

(2) The fracture toughness of coal shows strong anisotropic characteristics at different bedding angles during three point bending tests. Bedding has a weak ability to prevent fracture initiation and propagation. The specimen rupture modes basically show two failure types.

(3) The hydraulic fracture initiates at the end of perforation due to tension fracturing, and it generates induced fractures at the bedding. The bifurcation and diversion of major fractures take place at the bedding during further extension. More newly induced fractures are formed, creating a complicated fracture network which achieves the purpose of CBM reservoir fracturing treatment.

(4) The fracture toughness of bedding has great influence on hydraulic fracture geometry. The fracture is likely to bifurcate and swerve at the bedding to form multiple secondary fractures with larger bedding fracture toughness, which is beneficial to form a fracture network.

- Han, F. S., Busch, A., Krooss, B. M., Liu, Z. Y., Wageningen, N. V. and Yang, J. L., Experimental study on fluid transport processes in the cleat and matrix systems of coal. *Energ. Fuel.*, 2010, **24**, 6653–6661.
- Pan, R. K., Cheng, Y. P., Yuan, L., Yu, M. G. and Dong, J., Effect of bedding structural diversity of coal on permeability evolution and gas disasters control with coal mining. *Nat. Hazards*, 2014, **73**(2), 531–546.
- Claesson, J. and Bohloli, B., Brazilian test: stress field and tensile strength of anisotropic rocks using an analytical solution. *Int. J. Rock Mech. Min. Sci.*, 2002, **39**, 991–1004.
- Zhang, Z. T., Zhang, R., Li, G., Li, H. G. and Liu, J. F., The effect of bedding structure on mechanical property of coal. *Adv. Mater. Sci. Eng.*, 2014, **2014**, 1–7.
- Grasselli, G., Lisjak, A., Mahabadi, O. K. and Tatone, B. S. A., Influence of pre-existing discontinuities and bedding planes on hydraulic fracturing initiation. *Eur. J. Environ. Civ. Eng.*, 2015, **19**(5), 580–597.
- Li, Z. *et al.*, Propagation of hydraulic fissures and bedding planes in hydraulic fracturing of shale. *Chin. J. Rock Mech. Eng.*, 2015, **34**(1), 12–20.
- Jeffrey, R. G., Weber, C. R., Vlahovic, W. and Enever, J. R., Hydraulic fracturing experiments in the great northern coal seam. In SPE Asia Pacific Oil and Gas Conference, Melbourne, Australian, 7–10 November 1994.
- Gu, H., Siebrits, E. and Sabourov, A., Hydraulic-fracture modeling with bedding plane interfacial slip. In SPE Eastern Regional/AAPG Eastern Section Joint Meeting, Pittsburgh, PA, United States, 11–15 October 2008.
- Cho, J. W., Kim, H., Jeon, S. and Min, K. B., Deformation and strength anisotropy of Asan gneiss, Boryeong shale, and Yeoncheon schist. *Int. J. Rock Mech. Min. Sci.*, 2012, **50**, 158–169.
- Liu, K. D., Liu, Q. S., Zhu, Y. G. and Liu, B., Experimental study of coal considering directivity effect of bedding plane under Brazilian splitting and uniaxial compression. *Chin. J. Rock Mech. Eng.*, 2013, **32**(2), 308–316.
- Guo, T. K., Zhang, S. C., Qu, Z. Q., Zhou, T., Xiao, Y. S. and Gao, J., Experimental study of hydraulic fracturing for shale by stimulated reservoir volume. *Fuel*, 2014, **128**, 373–380.
- Heng, S., Guo, Y. T., Yang, C. H., Daemen, J. J. K. and Li, Z., Experimental and theoretical study of the anisotropic properties of shale. *Int. J. Rock Mech. Min. Sci.*, 2015, **74**, 58–68.
- Jiang, T. T., Zhang, J. H. and Wu, H., Experimental and numerical study on hydraulic fracture propagation in coalbed methane reservoir. *J. Nat. Gas Sci. Eng.*, 2016, **35**, 455–467.
- Ma, Y., Pan, Z. J., Zhong, N. N., Connell, L. D., Down, D. I., Lin, W. L. and Zhang, Y., Experimental study of anisotropic gas permeability and its relationship with fracture structure of Longmaxi Shales, Sichuan Basin, China. *Fuel*, 2016, **180**, 106–115.
- Zou, Y. S., Ma, X. F., Zhang, S. C., Zhou, T. and Li, H., Numerical investigation into the influence of bedding plane on hydraulic fracture network propagation in shale formations. *Rock Mech. Rock Eng.*, 2016, **49**, 3597–3614.
- Tang, C. A. and Hudson, J. A., *Rock Failure Mechanisms Explained and Illustrated*, CRC Press, 2010.
- Fakhimi, A. and Wan, F., Discrete element modeling of the process zone shape in mode I fracture at peak load and in post-peak regime. *Int. J. Rock Mech. Min. Sci.*, 2016, **85**, 119–128.

18. Googarchin, H. S. and Ghajar, R., Stress intensity factors calculation for surface crack in cylinders under longitudinal gradient pressure using general point load weight function. *Fatigue Fract. Eng. M.*, 2014, **37**(2), 184–194.
19. Heng, S., Yang, C. H., Guo, Y. T., Wang, C. Y. and Wang, L., Influence of bedding planes on hydraulic fracture propagation in shale formations. *Chin. J. Rock Mech. Eng.*, 2015, **34**(2), 228–237.
20. Sih, G. C., Pairs, P. C. and Irwin, G. R., On cracks in rectilinearly anisotropic bodies. *Int. J. Fract. Mech.*, 1965, **1**(3), 189–203.
21. Dai, F. and Xia, K. W., Laboratory measurements of the rate dependence of the fracture toughness anisotropy of Barre granite. *Int. J. Rock Mech. Min. Sci.*, 2013, **60**, 57–65.
22. Ministry of Water Resources of the People's Republic of China, *Specifications for Rock Tests in Water Conservancy and Hydroelectric Engineering*, China Standards Press, Beijing, 2007.
23. Chong, K. P., Kuruppu, M. D. and Kuszmaul, J. S., Fracture toughness determination of layered materials. *Eng. Fract. Mech.*, 1987, **28**(1), 43–54.

ACKNOWLEDGEMENTS. This research was funded by the China Postdoctoral Science Foundation Funded Project (No. 2016M592402), Hubei Provincial Natural Science Foundation of China (Nos 2016AHB015, 2016CFA013), and Wuhan Science and Technology Bureau (No. 2016070204020156).

Received 9 January 2017; revised accepted 21 April 2017

doi: 10.18520/cs/v113/i06/1153-1159

Deformational characteristics of Donglingxin slope induced by reservoir fluctuation and rainfall

J. Yu¹, R. B. Wang^{1,*}, J. C. Zhang², L. Yan¹, Q. X. Meng¹, C. Zhang¹ and X. Z. Li³

¹Research Institute of Geotechnical Engineering, Hohai University, Nanjing 210098, China

²College of Water Conservancy and Hydropower Engineering, Hohai University, Nanjing 210098, China

³Zhongnan Engineering Corporation Limited, PowerChina, Changsha 410014, China

Landslides induced by reservoir inundation and rainfall are very common in southwest China, adversely affecting the construction of hydropower plants in this area. In this study, a case of Donglingxin slope located at the Sanbanxi reservoir is reported, which developed into a large landslide. To understand deformation and conduct stabilization measurement, an in-depth study has been done based on monitoring the trigger events like reservoir fluctuation, rainfall and groundwater levels. It was revealed that the rainfall mainly affected deformation of the upper slope; reservoir fluctuation

reduced the stability of the toes of the slope. The activity of groundwater between the bedrock and the soil-rock mixture, geomaterials greatly controlled the global stability. An analysis of the comprehensive effects of these trigger events, indicated that the slope was unstable and would have slid into the reservoir. The evolution of slope deformation was simulated by particle flow code, the result showed that the landslide started from the head of the gully. This case study provides important geo-technical references for engineering the prevention of reservoir bank slopes.

Keywords: Donglingxin slope, deformational characteristics, reservoir bank slope, reservoir fluctuation, rainfall.

LANDSLIDE is one of the most serious geological hazards in the reservoir regions of hydropower station. Both reservoir fluctuations and rainfall infiltration become major factors that affect a landslide. Especially after impoundment, several ancient landslides are reactivated. Some huge reservoir landslide events have been previously reported¹. The Zhaxi landslide induced by a reservoir killed over 70 workers in 1961 (ref. 2). The Qianjiangping landslide, also induced by a reservoir killed 24 people in 2003 (ref. 3). So the stability of reservoir slope is a major problem in China and the economic losses related to landslide are over 20 billion every year⁴.

According to Qi *et al.*⁵, the mechanical strength of sliding zone controls the deformation of landslide, and hydraulic effects deteriorate the strength of sliding zone. Taking an example of Shuping landslide, Wang *et al.*⁶ found that the deformation of Shuping landslide corresponds to the Three Gorges reservoir fluctuations, especially, the deformation of the landslide is more active during periods of declining reservoir levels. Continuous rainfall also triggers the failure of slope, because the strength of the sliding zone is reduced by water infiltration⁷. Besides, Burda *et al.*⁸ proposed that the climate change induces reactivation of landslide.

The Donglingxin slope is an ancient landslide with a volume of 20.7 million m³. It is located on the right bank of Qingshui river, Guizhou Province (Figure 1). The slope belongs to Sanbanxi hydropower project, which is about 80 km downstream of the slope. In July 2007, during the first reservoir impoundment, the ancient landslide was reactivated. The valley in the landslide region is extremely narrow, hence the support and protection measurements are difficult to be implemented. As this landslide located only 1 km from Liuchuan town with more than 30,000 inhabitants, its stability is a major safety problem. Therefore, we must analyse landslide deformation characteristics and also its potential failure.

This communication presents a comprehensive analysis of Donglingxin landslide. Based on the two-year observation data, we analysed landslide deformation and triggering mechanism related to reservoir fluctuation and rainfall. The factor of safety is calculated for stability

*For correspondence. (e-mail: rbwang_hhu@foxmail.com)